Ecological Indicators 156 (2023) 111182

Contents lists available at ScienceDirect

Ecological Indicators

journal homepage: www.elsevier.com/locate/ecolind

Original Articles

Soil erosion susceptibility mapping in Bangladesh

Halima Sadia [a], Showmitra Kumar Sarkar [a,*], Mafrid Haydar [a]

[a] *Department of Urban and Regional Planning, Khulna University of Engineering & Technology (KUET), Khulna 9203, Bangladesh*

ARTICLE INFO

Keywords:
Data driven approach
Knowledge based approach
Machine learning
Remote sensing
Soil erosion

ABSTRACT

This study aims to draw a scientific framework for plotting soil erosion susceptibility in the Chittagong Hill Tracts of Bangladesh by comparing existing approaches. Data-driven machine learning techniques (including Classification and Regression Tree (CART), Artificial Neural Network (ANN), Support Vector Machine (SVM), and Random Forest (RF)) and a knowledge-based approach (AHP) are used in this study to pinpoint areas of Chittagong that are particularly susceptible to soil erosion while taking into account 18 soil erosion-regulating parameters. Furthermore, the effectiveness of the selected data-driven machine learning models and knowledge-based models was assessed by utilizing soil erosion and non-erosion sites. When evaluating the fidelity of each model using the ROC and AUC, the RF model was shown to be the most accurate and predictive. There is no poor performer among these models; all have AUCs greater than 67 % (RF = 0.86, ANN = 0.73, SVM = 0.67, CART = 0.67, and AHP = 0.82). According to the findings of the Random Forest model, approximately 71.55 percent of the area exhibited a moderate level of susceptibility to soil erosion. In relation to the land area, the high and low zones accounted for 16.91 percent and 11.54 percent, respectively. The specific area shares of 2256.25, 9548.08, and 1539.67 square kilometers were attributed to the high, moderate, and low danger zones, respectively. The best models' results after comparing models of data-driven and knowledge-based approaches can help to estimate soil erosion risk zones and provide insight into establishing appropriate policies to minimize this issue. In addition, the methods used in this research might be applicable to assessing the vulnerability and risk of soil erosion events in other areas. As they begin long-term planning to reduce soil erosion, local authorities and policymakers will find the study's results on practical policies and management options quite helpful.

1. Introduction

Soil erosion causes long-term losses in biodiversity and agricultural output that can't be restored without human intervention (Bai et al., 2008). Among the various factors influencing soil erosion are soil type, vegetation cover, soil topography, and natural hazards like earthquakes. Long, steep slopes are more prone to soil erosion than shorter, flatter ones (Rahman, 2021). The advancement of complex domains contributes to the emergence of environmental pollution, which in turn results in the phenomenon of climate change. Climate change is also an important issue when considering soil erosion and the first perceptible change in the formation of a region is its greenery, which influences its topography, morphology, climate, and distinctive structure. Often, there appears to be a lack of comprehension among persons regarding the core notion that soil erosion is an expected outcome resulting from poor land utilization, and that its rectification is contingent upon addressing errors in land use and management. The issue persists as a significant concern throughout the Asian mountain regions (Xu et al., 2013). The issue of soil erosion poses a significant challenge in Bangladesh, a developing country that is heavily dependent on agriculture as a key driver of its economy (Krishna Bahadur, 2009).

The Chittagong Hill Tracts (CHT) of Bangladesh are one of the most prominent examples of the consequences caused by soil erosion in tropical highland regions (Rahman, 2021). Erosion is one of eight soil dangers the European Commission tackles in its Soil Thematic Strategy, and it is called a "major threat" in the publication. In accordance with the RCP2.6, RCP4.5, RCP6.0, and RCP8.5 scenarios, the IPCC 5th Assessment Report projected total soil losses of 308.9, 323.5, 320.3, and 355.3 million tons between 2060 and 2080 (Berberoglu et al., 2020). Reports indicated that 35.72 percent of the areas were extremely hazardous, and 46.69 percent were extremely susceptible to erosion. Ranges from extremely high to high erosion risk were detected in a total of 45 unions out of the 161 coastal unions and their main islands. These unions are found along the shores of the districts of Bhola, Noakhali, and

* Corresponding author.
E-mail address: mail4dhrubo@gmail.com (S.K. Sarkar).

https://doi.org/10.1016/j.ecolind.2023.111182
Received 30 June 2023; Received in revised form 10 October 2023; Accepted 27 October 2023
Available online 31 October 2023

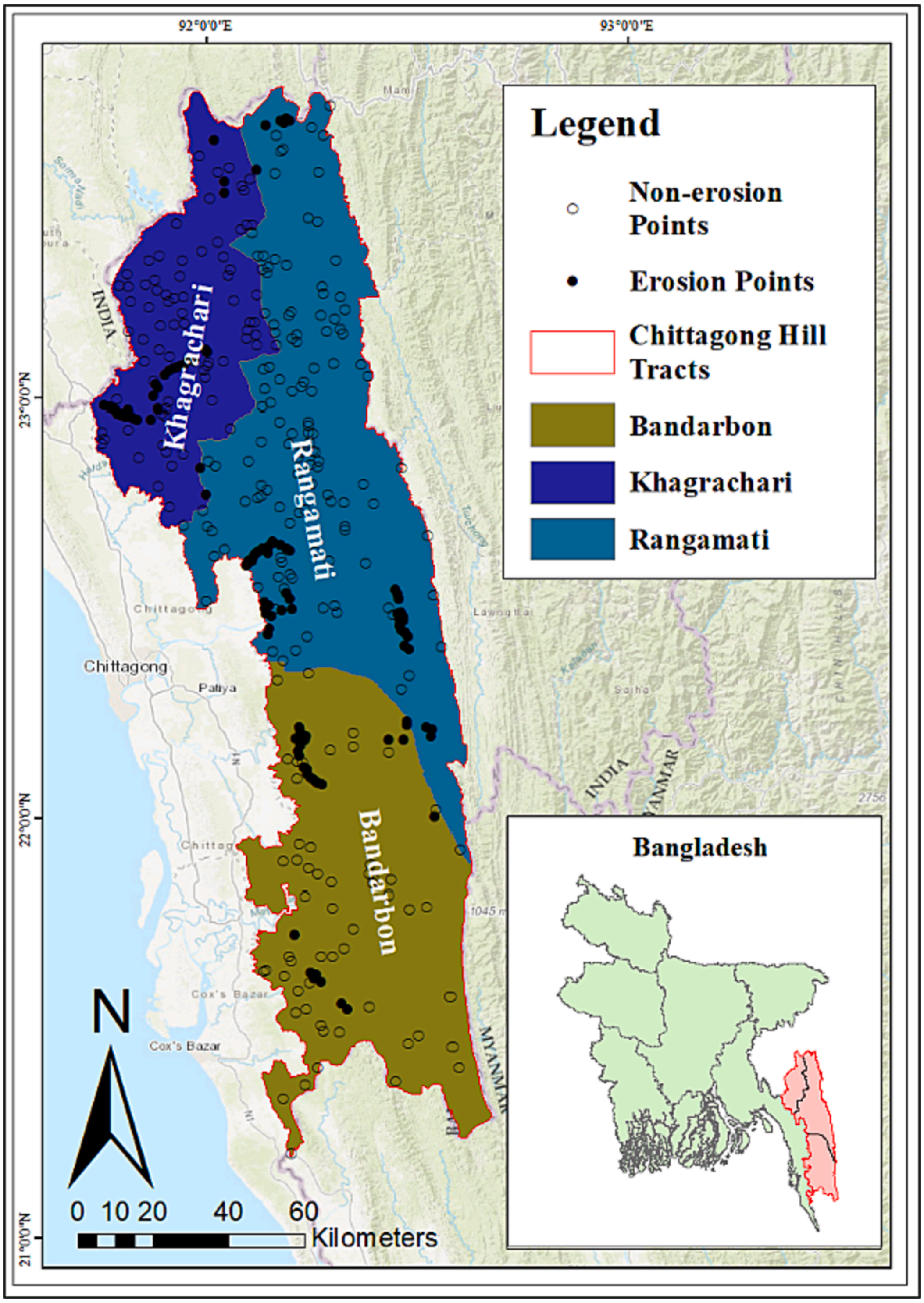

Fig. 1. Study area and Site Inventory map (Chittagong Hill Tracts).

Barishal In this data-driven and machine learning-based procedure, the data is divided into two sets: 70 % for training and 30 % for testing (Bai, 2006; Bai et al., 2008; Farid et al., 1995; Hasan and Ashraful Alam, 2006). The impact of soil erosion is beyond our imagination in terms of damage to fertile land. Soil erosion is also the cause of water pollution and sand sedimentation. As a result, the water ecosystem gets disturbed, and we see a decrease in fish production (Ahmed et al., 2020). CHT is also one of the most prominent nature-based tourist attractions in Bangladesh. Tourists should be carefully developed and managed for better economic flow and environmental protection. Soil erosion causes changes in streambed depth and water quality due to deposition. Flooding along the banks is substantially more severe due to the sedimentation of waterbodies. According to researchers, 43 % of the phosphorus in water is agriculturally produced as a consequence of soil erosion (Mardamootoo, 2015). Soil erosion in Bangladesh is estimated to be between 7 and 120 tons per acre per year, based on previous studies. Soil erosion is responsible for a staggering 50–60 tons per hectare per year (Roy et al., 2021). The erosion risk in hilly locations ranges from

Table 1
Data sources of soil erosion controlling parameters for soil erosion susceptibility.

Category		Sources	Resolution	Data type
Topographical Parameters	Elevation (DEM)	NASA Earth Data	30 × 30 m	Raster
	Slope	Extracted From DEM	30 × 30 m	Raster
	Plan Curvature	Extracted From DEM	30 × 30 m	Raster
Hydro-climatic Parameters	Drainage density	Extracted From DEM	30 × 30 m	Raster
	Flow accumulation	Extracted From DEM	30 × 30 m	Raster
	Flow direction	Extracted From DEM	30 × 30 m	Raster
	Stream Link	Extracted From DEM	30 × 30 m	Raster
	Stream Order	Extracted From DEM	30 × 30 m	Raster
	Watershed	Extracted From DEM	30 × 30 m	Raster
	TWI	Extracted From DEM	30 × 30 m	Raster
Land-cover Parameters	Soil Brightness Index	Sentinel − 2	10 × 10 m	Raster
	NDVI	Landsat − 8	30 × 30 m	Raster
	LULC	Landsat − 8	30 × 30 m	Raster
Geological Parameters	Roughness	Extracted From DEM	30 × 30 m	Raster
	Lineament density	Extracted From DEM	30 × 30 m	Raster
	Soil Erosion inventory	Literature Review, Google earth imageries, Newspaper.		Vector

"extreme" (75 %), "high" (20 %), and "moderate" (5 %) to "low (Hasan and Ashraful Alam, 2006). Over the previous 20 years, due to intensive agricultural practices, the average organic matter content of upper soils (high land and medium–high land conditions) has dropped from around two to one percent (M. R. Islam et al., 2010). The worldwide loss of farmland is mostly attributable to soil erosion. Identification of regions that are especially prone to erosion in the future is crucial due to the damaging effects of soil erosion (Nearing et al., 2017). Due to commercial activity, land usage is fast shifting in Chittagong's hill tracts. Thus, change in land use tends to cause more soil erosion than previous times. Reduces land productivity, affects agricultural sustainability, and affects the quality of soil, air, and water, indirectly decreasing environmental quality. Combining a machine learning-based approach with GIS will enhance the chances of mapping the soil erosion-prone region more accurately while creating opportunities to mitigate the damage of the Chittagong hill tracts.

Erosion of soil caused by human activities is becoming a more serious issue in the littoral areas of southeast Bangladesh. Purportedly evicted Myanmar Nationals, commonly known as "Rohingya," eluded Myanmar in 2017. Since then, soil degradation in the area has escalated. The first step in effective soil erosion management is the location and severity assessment of erosion hotspots. In this endeavor, an effort was made to evaluate regional soil loss (from 2015 to 2020) using the RUSLE model (Hossain et al., 2022). Steep slopes, unstable soils, and frequent monsoon rainfall characterize the CHT region, which includes districts such as Rangamati, Bandarban, and Khagrachhari. Deforestation, shifting farming patterns, poor land management, and infrastructural development are the primary reasons for soil erosion in this region. Mountainous terrain and heavy rainfall accelerate erosion, resulting in landslides, river sedimentation, and the loss of fertile topsoil (Hasan and Ashraful Alam, 2006). Only 18 % of Bangladesh consists of hilly and tractable terrain; however, this is where a substantial portion of the population presently dwells as a result of rapid urbanization (Ravenscroft et al., 2005). About 10 % of Bangladesh's total landmass is inside the CHT's boundaries. More than 70 % of the land inside the CHT has an inclination of more than 40 %, making it rather steep in comparison to the low-lying floodplains that make up the bulk of Bangladesh. The soil is not very fertile. Kyokra-Dong is the highest peak in Bangladesh at 1,230 m, and it may be found in the southernmost part of the Rangamati district, not far from the borders with India and Myanmar (Mantel & Khan, 2006). According to studies, the watershed has an annual soil erosion rate of 14.98 tons per hectare, with a maximum rate of 1,436.10 tons per hectare (Rahman, 2021). A physical investigation revealed that the alluvial, silty clay soil characteristic of the Chittagong Hill Tracts (CHT) is prone to landslides. Over the last half-century, CHT has been hit by around a dozen major avalanches. The most subversive landslides on record occurred in 2007 and 2017 (A. Islam & Islam, 2017). Using a GIS-based multi-criteria decision approach, soil erosion susceptibility mapping in Chitral, Pakistan reveals five distinct classes, including very high, high, medium, low, and very low. 13 % and 18 % of the total study area exhibit very high and high levels of soil erosion, respectively, indicating that this region is in grave peril of soil erosion. Elevation, slope, curvature, NDWI, and precipitation have been identified as the most influential factors in the soil erosion process (Aslam et al., 2021).

Soil erosion is a widely recognized and significant issue in this particular area, which imposes constraints on the feasibility of land-use practices that are environmentally sustainable. Therefore, the identification and delineation of areas susceptible to soil erosion holds significant importance in this particular location. The availability of accurate quantitative data of this nature can serve as a crucial element in the development and implementation of successful and sustainable strategies for soil and water management on a global scale. Numerous research endeavors have been conducted to delineate the susceptibility of landslides; nevertheless, there is a dearth of studies that have specifically concentrated on assessing the susceptibility of soil erosion. Previous studies on landslide susceptibility have employed various methodologies to assess and analyze this phenomenon. Qualitative approaches, such as Analytic Hierarchy Process (AHP) and Weighted Linear Combination (WLC), have been utilized. Bivariate techniques, such as Weight of Evidence (WoE), have also been employed. In addition to that, multivariate statistical approaches have been utilized, such as logistic regression. There have also been uses of methods from the field of machine learning, such as support vector machines. Additionally, hybrid models, such as the frequency ratio technique, have been developed and are currently being utilized within the scope of this discussion. There has not been a sufficient amount of research conducted to either validate the models or undertake a comparison study of the outputs of the models in order to determine which susceptibility map is the most accurate. Both of these steps are necessary in order to find the most accurate map of susceptibility. In addition, there is a substantial disparity between the effectiveness of mapping soil erosion susceptibility accomplished by models that are based on knowledge as compared to models that are driven by data when it comes to the mapping of soil erosion susceptibility.

This research aims to provide a map of the Chittagong Hill Tracts' erosion risk. The following targets can be assessed in light of this: (i) To investigate the conditions of different soil erosion parameters (i.e., Topographical parameters, Land cover parameters, Geological Parameters, Hydro-climatic parameters) in Chittagong hill tracts; (ii) To assess soil erosion susceptibility zones utilizing data-driven structures such as RF, CART, SVM, ANN, and knowledge-based models (AHP); (iii) To compare among data-driven models and knowledge-based models for soil erosion susceptibility in CHT.

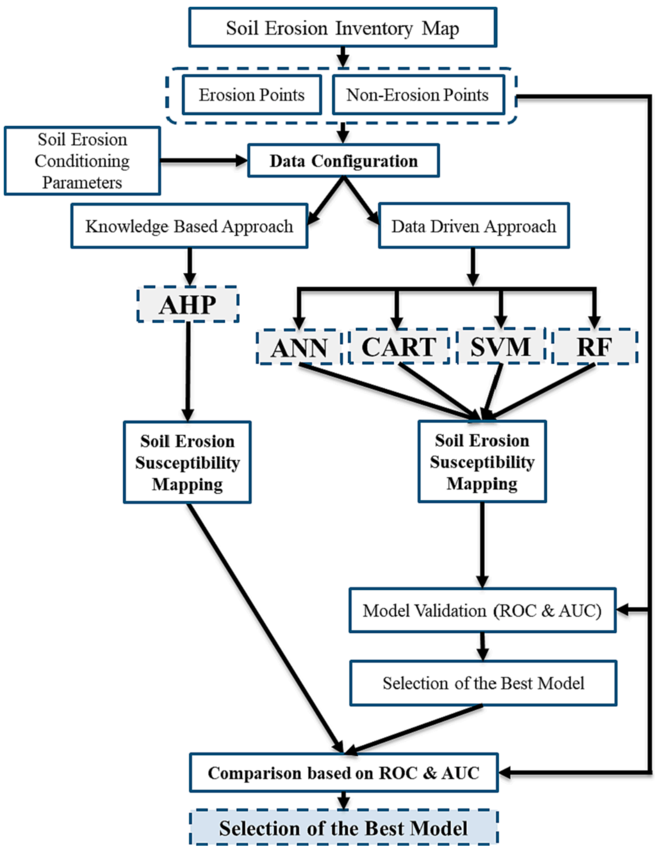

Fig. 2. Conceptual and methodological framework for the study.

2. Methods and materials

2.1. Description of the study area

The Chittagong Hill Tract is the site of the inquiry (Fig. 1). Located in southeastern Bangladesh, the Chittagong Hill Tracts (CHT) are made up of the hill districts of Rangamati, Bandarban, and Khagrachari. Its 13,294 square kilometers are almost entirely mountainous. According UNICEF, 2019, the population is 1.6 million. The city of Rangamati is in Bangladesh's southeastern corner. The coordinates 22° 38′ N and 92° 12′ E pinpoint the research zone. You may find forests, rocky and earthy slopes, cascades, rivulets (chara), and river gorges. In between the mountain ranges are narrow stretches of flat land. The soil in the Rangamati mountains drains well, while the muddy soils in the valley are poorly drained and often get flooded (Huq et al., 2013). Because of its position, peculiar geomorphic features, and heavy precipitation, this area is one of the most prone to landslides in Bangladesh (Mia et al., 2015). It is possible to classify the region's mountains as either low (300 m) or high (300 m +). The Dupi Tila and Dihing formations support the low hill ranges, while the Surma and Tipam formations support the high hill ranges. Slopes less than 5 degrees are typical in the west, whereas those more than 30 degrees are typical in the east (Rasul et al., 2004; Saha et al., 2004).

2.2. Description of data

The initial data gathering and subsequent construction of thematic layers were conducted inside a Geographic Information System (GIS) and remote sensing environment (Table 1). As remote sensing is widely utilized to assess the changing dynamics of ecosystems and environment (Abad-Segura et al., 2020; S. K. Sarkar et al., 2022). Subsequently, we identified the influencing and dependent variables pertaining to soil erosion issues. In this study, complex methods including Support Vector Machines (SVM), Random Forest (RF), Classification and Regression Trees (CART), and Artificial Neural Networks (ANN) were employed to construct more intricate models for predicting soil erodibility and susceptibility. By employing these models, which included a knowledge-based approach based on the Analytic Hierarchy Process (AHP), the production of maps depicting soil erosion hazards was facilitated. In order to select the most optimal model from a range of data-driven approaches, the process of ROC-AUC curve validation is conducted. Subsequently, the models of both strategies were evaluated and contrasted through the use of the Receiver Operating Characteristic - Area Under the Curve (ROC-AUC) analysis.

2.2.1. Inventory of soil erosion

Eventually, the model's calibration and validation have been

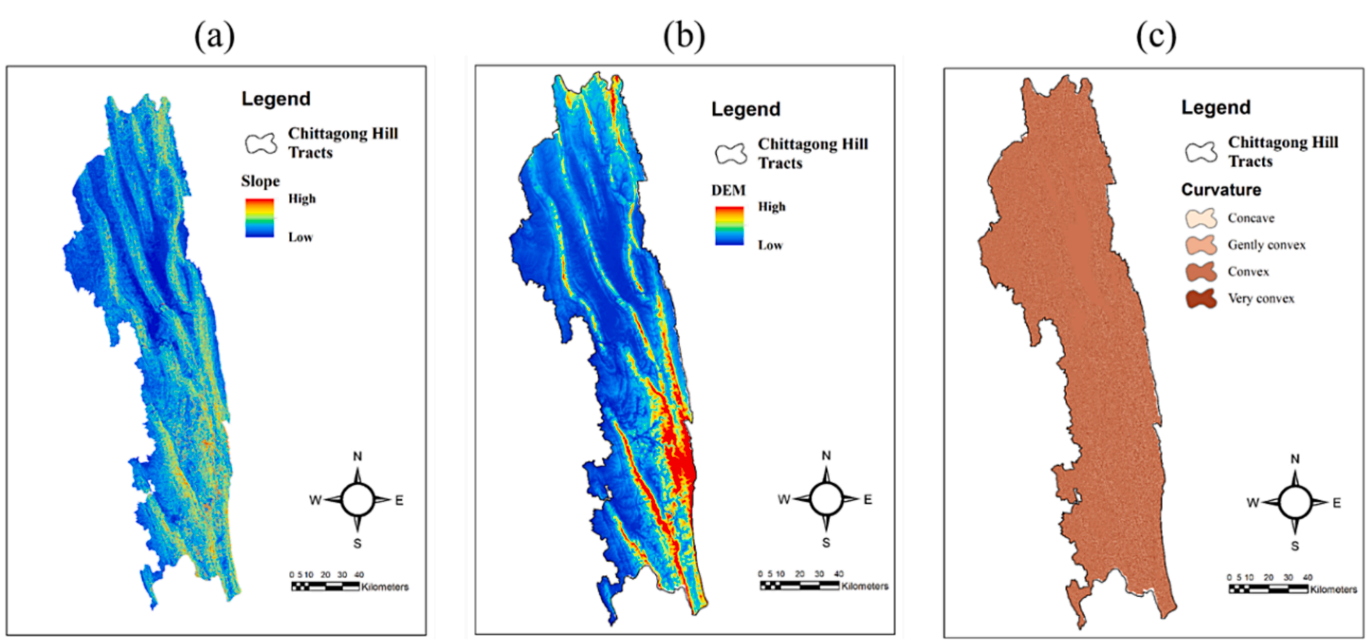

Fig. 3. Topographical Parameters (a) Slope, (b) Elevation, (c) Plan curvature.

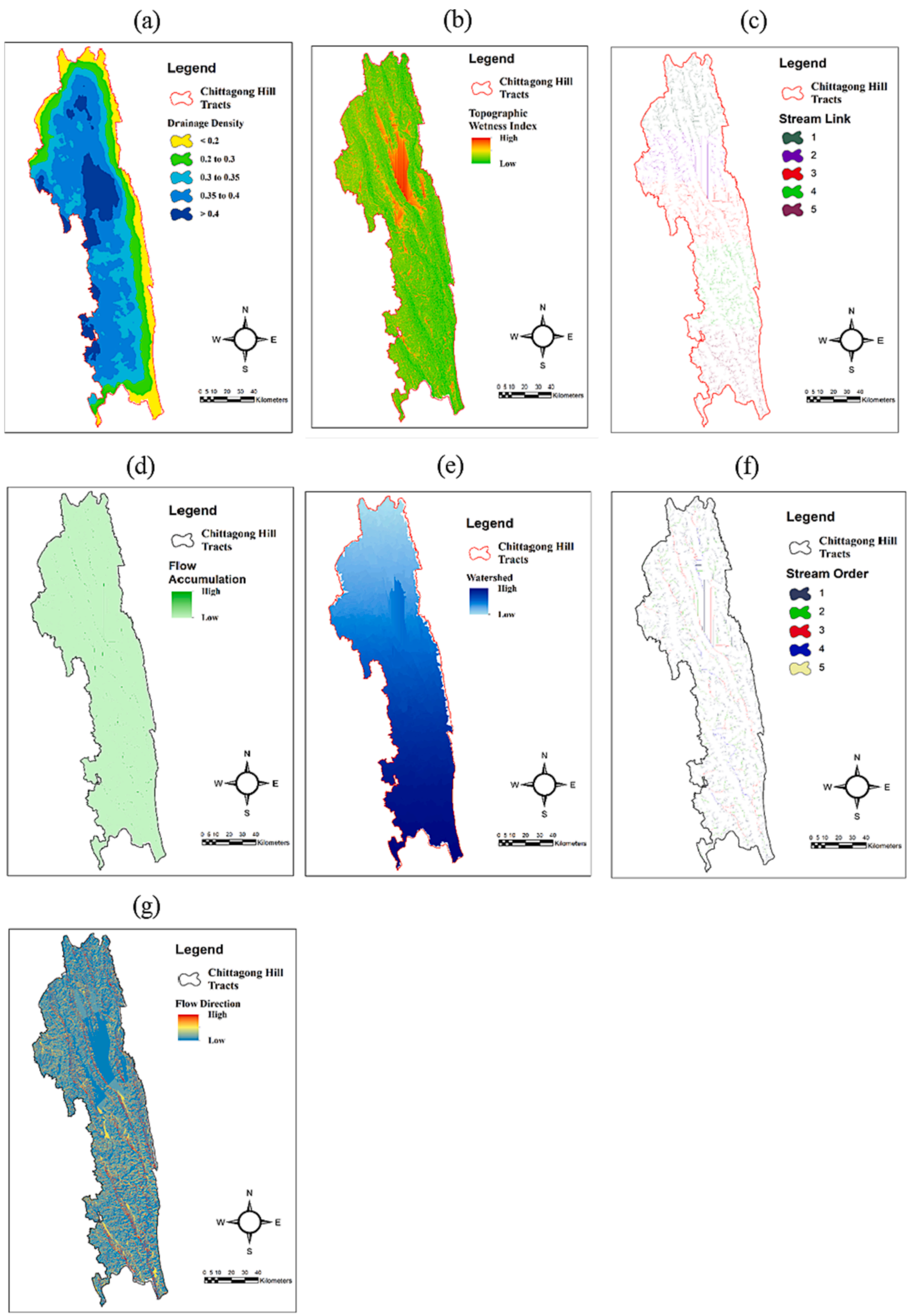

Fig. 4. Hydro-Climatic Parameters (a) Drainage density, (b) Topographic wetness index, (c) Stream Link, (d) Flow accumulation, (e) Watershed, (f) Stream order, (g) Flow direction.

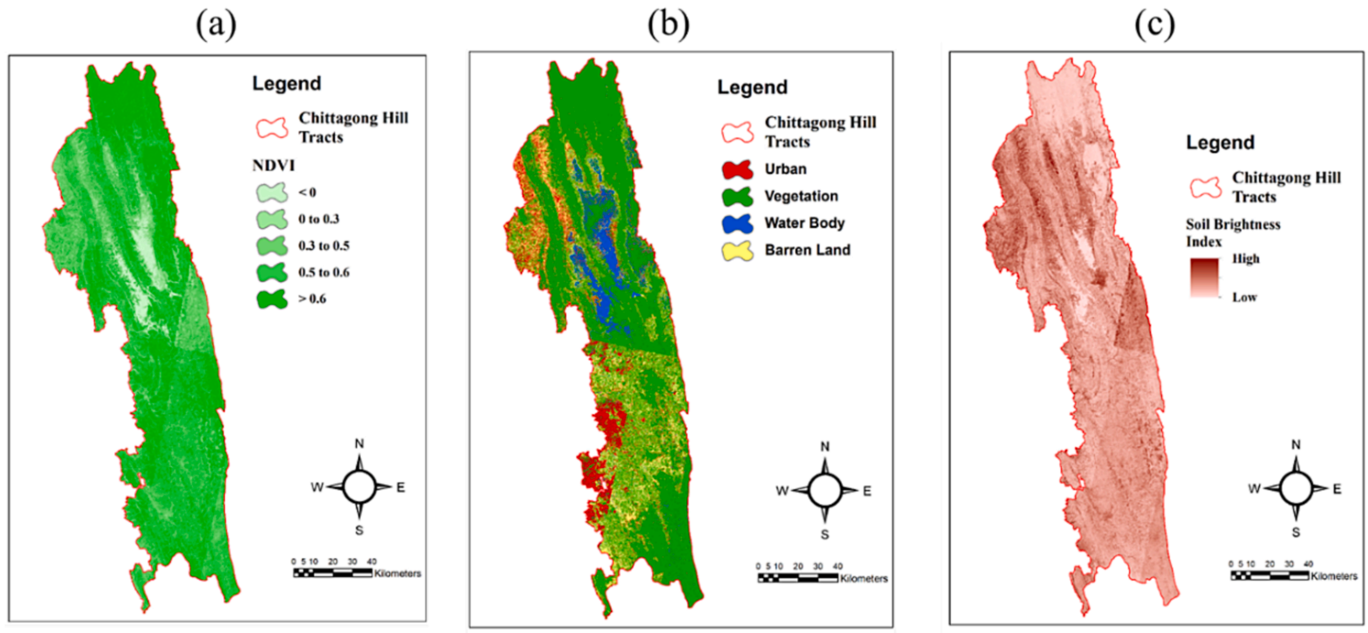

Fig. 5. Land cover Parameters (a) NDVI, (b) LULC, (c) Soil Brightness Index.

completed using data from 119 erosion locations and 252 non-erosion points. Detailed literature analysis, high-resolution satellite pictures, Google Earth imagery, and recent erosion occurrences were used to select 119 erosion spots for the calibration as well as the validation of the model, while random sampling was used to sample the other 252 places.

2.2.2. *Anticipation of the factors driving soil erosion*

In this study, we obtained maps using the following spatial dataset: Data from the 30 m SRTM DEM (Digital elevation model) is useful for a wide variety of applications, including but not limited to slope preparation, LS, DD, TWI, FA, Landsat 7 ETM + and Landsat 8 (OLI) pictures, Geological Maps, Lineament Layer, Soil Texture Map, Hydrological Soil Groups (HSG) Map, and Lineament Density Map. Multiple data stores may be queried for information. Soil erosion rates vary depending on local geological and environmental conditions. The researchers took into account a wide range of topographical, hydrological, morphological, and soil-related factors, including elevation, slope, plan curvature, stream density, stream order, drainage density, topographic wetness index, flow accumulation, and flow direction.

2.2.3. *Topographical parameters*

Plant distribution, physiology, and development are all affected by soil erosion, which is modeled by the Digital Elevation Model (DEM) (Halefom & Teshome, 2019). Both temperature and plant life are affected by elevation. Until a certain altitude, when the quality of the rock and soil and other geotechnical criteria make further soil erosion less likely, soil erosion rates tend to rise as elevation increases. The slope is an important topographical feature that influences soil stability. Transportation of sediment and runoff in a basin is affected by this (Vemu & Udayabhaskar, 2010). A higher slope increases the risk of soil erosion, whereas a gentler one enhances the channel's carrying capacity. The ASTER DEM served as the basis for ArcGIS's slope raster. The ground's curvature is crucial in identifying erosion-prone areas because it controls the convergences and divergences of downslope water fluxes and influences the processes of surface runoff and sediment transport. When a horizontal plane cuts over the surface at right angles to the direction of greatest slope, we get planar curvature, as described by Mosavi et al. in 2020. The curvature of this plane determines the contour line's form (Shit et al., 2015). Each cell's convexity and lateral concavity, for example, are given numerical values (positive for convexity and negative for lateral concavity). In order to create the curved map, ArcGIS and SRTM-DEM data were used.

2.2.4. *Hydro-Climatic parameters*

The likelihood of erosion varies from place to place due to differences in drainage. Permeability, surface resistance, and soil depth (Shamshirband et al., 2020) all have an effect on drainage density (DD). There was greater surface runoff when there were more drains per unit area (Arabameri et al., 2018). Consequently, regions with a high drainage density are more likely to experience soil erosion (Mosavi et al., 2020) and contribute to a basin's sediment output (Mustafa et al., 2018) than those with a low drainage density. ArcGIS was used to determine the density of drainage and the length of streams. The stream network was extracted from SRTM-DEM (1 arc second) data using Arc Hydro methods. Drainage density was then created using ArcGIS's line frequency and distance from Euclid tools. A channel, also known as a watercourse connection, can significantly influence soil erosion. When water flows down a stream channel, it can erode the sediment and transport it downstream. Stream connections can also contribute to erosion by altering the movement of water across the landscape (Sweeney et al., 2004). For example, increasing the width or depth of a stream channel can enhance the volume and speed of water flow. This increased flow may result in additional erosion and silt transfer, further degrading the surrounding soil. Stream order is the hierarchy of streams and rivers within a drainage basin, with the tiniest first-order streams and the greatest highest-order streams (Shit et al., 2015). The influence of stream order on soil erosion varies depending on a number of variables, including geography, land use, and climate. In general, higher-order streams are more likely to have a greater influence on soil erosion due to their larger drainage area and consequently greater capacity to convey sediment downstream (Römkens et al., 2002). However, the effect of stream order on soil erosion is also ascertained by parameters such as topography, steepness and soil type. The slope and upstream contributing area per unit width orthogonal to the flow direction form the basis of the Topographic wetness index (TWI). Soil and rainfall patterns affect TWI (Pradhan & Kim, 2020). The geographical distribution of runoff sources and saturation zones is described, as is the effect of topographic changes on soil runoff (Mosavi et al., 2020; Xiao et al., 2021). A bigger discharge capacity corresponds to a higher

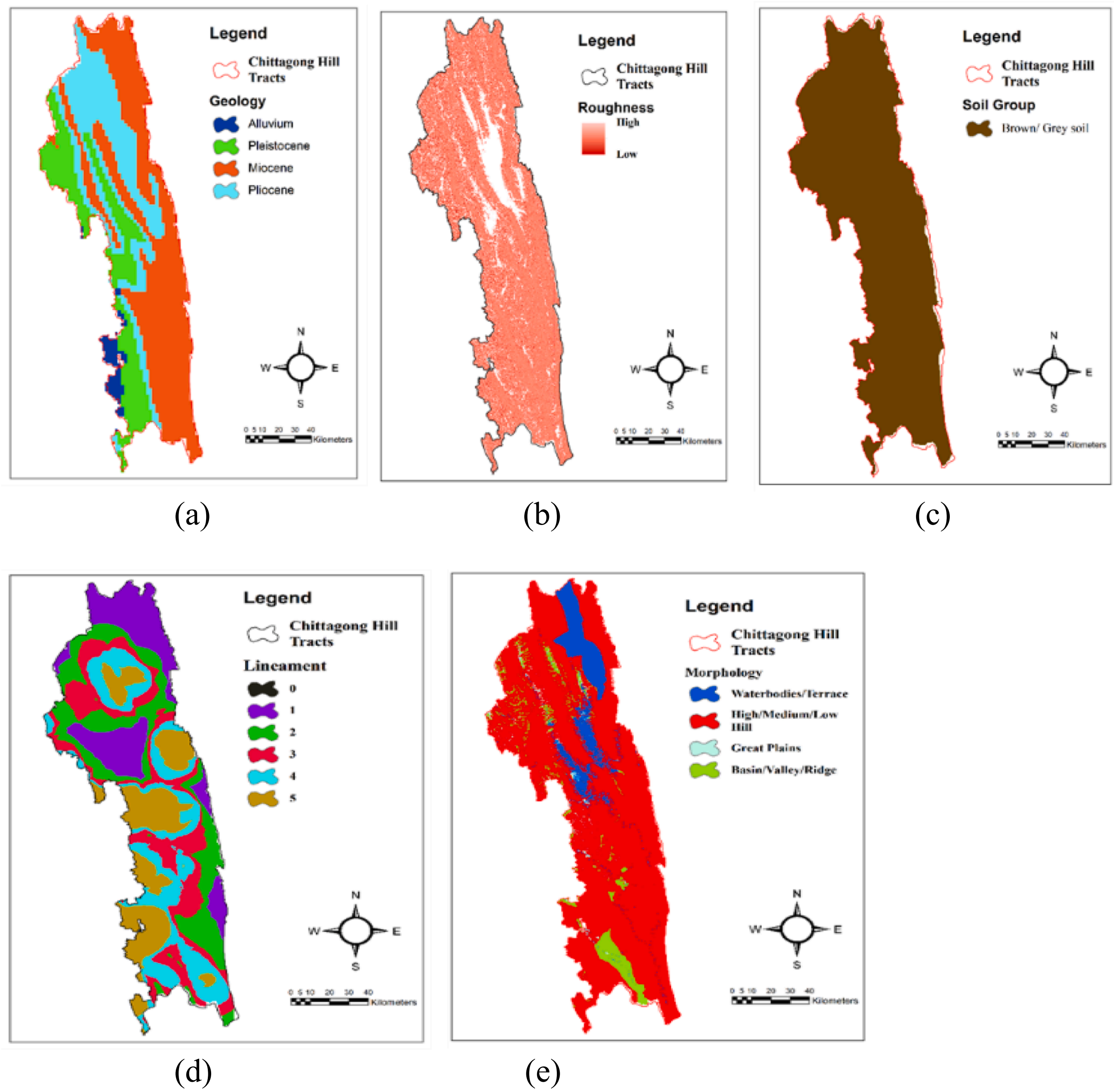

Fig. 6. Geological Parameters (a) Geology, (b) Roughness, (c) Soil Group, (d) Lineament density, (e) Morphology.

number, and vice versa. Soil moisture, total water storage, and a representation of the basin's soil humidity are all shown by this component (Halefom & Teshome, 2019). Using SRTM-DEM and the Moore et al. (1991) method, TWI values were determined. The number of cells that enter a cell is used to get the flow accumulation (FA) value. Each cell's value in the resultant raster is the sum of the cumulative weights of each cumulative pixel, which indicates the total amount of water that flows downstream from the corresponding cell in the upstream raster. When a lot of SE-affected pixels accumulate in a river's flow water, it's easy to make runoff (Mosavi et al., 2020). The zone of concentrated flow is defined by the cells that experience the greatest amount of flow and is used to determine the stream's channel. Local topographic highs can be characterized by using cells with zero flow buildup. The SRTM-DEM Arc Hydro tools were used to generate the FA raster, which was then combined with a simple D8 flow direction algorithm. Dirt erosion occurs when dirt travels in the direction of water flow, which has a significant impact on soil erosion. One location to another due to an act of water or wind. When water flows over the soil surface, it can pick up soil particles and carry them downstream, resulting in soil erosion. The direction of water flow determines which portions of the soil are most susceptible to erosion. When water runs downhill, the soil at the bottom of the slope erodes faster than the soil at the top. This is because water runs faster and has more energy near the bottom of the slope, forcing it to pick up and transport more soil particles (Lohani et al., 2020). The flow of water can influence where these channels form and how quickly they grow. The characteristics of the watershed affect soil erosion in hilly areas. The watershed, which is defined as the area of land where all water descends into a single outlet such as a river or lake, affects water flow, sediment transport, and erosion patterns (Amarakul, 2001a; Ghorbanzadeh et al., 2020). Watersheds are responsible for determining the patterns of water

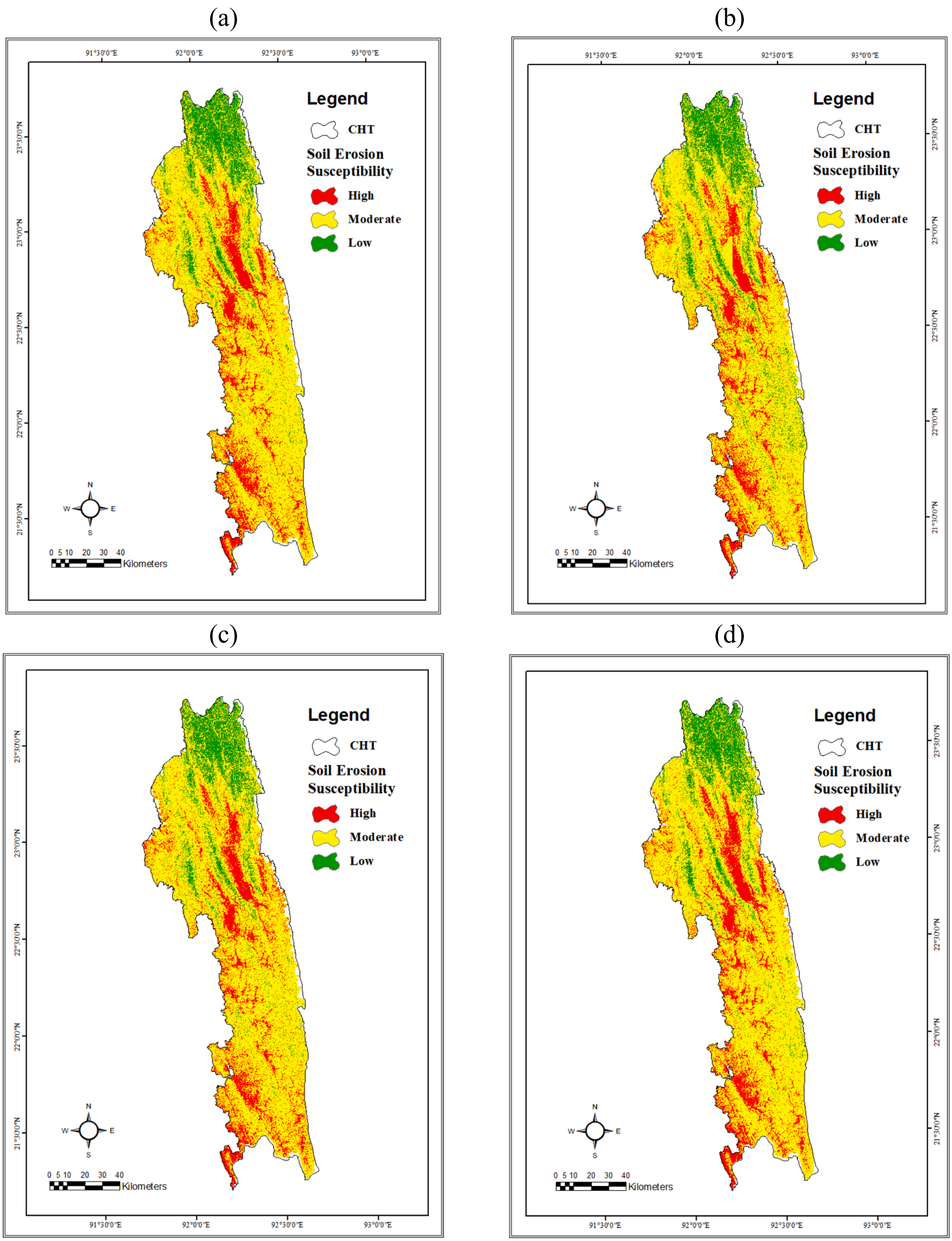

Fig. 7. Soil Susceptibility Maps by Data Driven Approach (a)ANN, (b) CART, (c) RF, (d) SVM.

Table 2
Area & Percentage of susceptibility categories in different data driven models.

Method	High		Moderate		Low	
	Area (sq. km)	%	Area (sq. km)	%	Area (sq. km)	%
RF	2256.25	16.91	9548.08	71.55	1539.67	11.54
SVM	2361.09	17.69	9420.60	70.60	1562.31	11.71
CART	2150.01	16.11	9321.38	69.85	1872.62	14.03
ANN	2284.03	17.12	9454.74	70.85	1605.23	12.03

Table 3
Weight and ranks of the soil erosion parameters.

Parameters	Weight/Influence	Rank
Elevation	13	1
Topographic wetness index	12	2
Slope	11.2	3
Watershed	10	4
Drainage density	8	5
NDVI	6	6
Soil Brightness Index	6	7
Lineament density	6	8
Plan curvature	5	9
Flow accumulation	5	10
Roughness	5	11
Flow Direction	4	12
LULC	4	13
Geology	3	14
Stream Link	0.6	15
Stream Order	0.6	16
Soil group	0.3	17
Morphology	0.3	18

discharge across the landscape. Watersheds in mountainous terrain may contain multiple streams and channels that collect and transport water downward. The size and structure of the watershed affect the quantity and intensity of discharge produced during storm events. Higher discharge volumes and velocities are produced in watersheds with steeper slopes and fewer drainage areas, which increases the likelihood of soil erosion (Tehrany et al., 2017).

2.2.5. Land cover parameters

The Normalized Difference Vegetation Index (NDVI) is used to quantify plant cover (Mandal & Sharda, 2013; Razavi-Termeh et al., 2020). One possible value for the NDVI is + 1. The thick and vigorous vegetation is indicated by the high NDVI rating. In general, thick vegetation cover helps minimize soil erosion by reducing surface runoff and keeping soil in place through plant roots (Arabameri et al., 2018). This means that areas with high NDVI values are more resistant to soil erosion (Mosavi et al., 2020) and experience less soil erosion (Avand et al., 2023). Landsat 8 (OLI) satellite images were used to derive NDVI values using the following equation. Reflectance spectrum are often broken down into two categories: near-infrared (NIR) and red (visible) (Mosavi et al., 2020). The processes of surface discharge, infiltration, and evapotranspiration are affected by the ways in which land is used and covered (Ouri et al., 2020). Forests and grasslands provide a natural barrier to water and wind, reducing the likelihood of soil erosion (Ahmad & Goparaju, 2017). In contrast, soil erosion is exacerbated by surface discharge, which is increased on fallow and barren surfaces. Effective management of the land, taking into consideration its potential and restrictions, is necessary to prevent excessive soil erosion (Panwar & Singh, 2014). Using Landsat 8 (OLI) 2021 data, the LULC map of the study area was constructed using the greatest likelihood method. The LULC was separated into four zones: populated regions, greenery, bodies of water, and bare ground. Bare, waste, or exposed surfaces account for around 21.29 percent of the land, making it very vulnerable to erosion of soil. El Jazouli et al. (2017) found that the Soil Brightness Index (SBI) can define difference between soil with and without vegetation. Soil erosion is more harmful on exposed areas with little or no protection, as opposed to fortified terrain (Chakrabortty et al., 2020). A high brightness index has the opposite effect, encouraging barren soil and granite over vegetation. Using Google Earth Engine and Landsat 8 (OLI) satellite data, we calculated the SBI using the following methods.

2.2.6. Geological parameters

Soils in the CHT are commonly classified as HSG A (high infiltration rates with low runoff potential) or HSG B (moderate infiltration rates with moderate runoff potential). There are, however, locations with HSG C and D soils, which have low infiltration rates and significant runoff potential, rendering them very prone to erosion (Lohani et al., 2020). In hilly regions, the soil undergoes a constant process of recycling and transformation, wherein ancient rocks are broken down into particles of sand, silt, and clay. The transformation of urban environments as a result of human activities, along with the influence of micro-ecological factors, has a significant impact on the modification of soil structure. When these soils are subjected to heavy precipitation, the discharge can quickly cause soil erosion and sedimentation, damaging the natural environment and disrupting local communities that rely on the land for agriculture and livelihoods. Geological factors may have a significant role in soil erosion. One of the major factors in soil erosion is the soil's capacity to retain water. Sandstone and shale, which are porous and allow water to quickly pass through them, can result in soil that is less able to hold water. This can cause the soil to dry out quickly, increasing its vulnerability to erosion during periods of heavy rain or strong winds. Soil erosion is also influenced by climate. High rainfall or frequent storms increase the likelihood of erosion since the water can readily wash away the top layer of soil. Erosion of soil can be greatly triggered by geology (Amarakul, 2001b). The soil's capacity to retain water is one of the most dominant factors that contribute to erode soil. Sandstone and shale, which are permeable and enable water to pass through them rapidly, can result in soil that is less capable of retaining water. This can cause the soil to dry out rapidly, making it more susceptible to erosion during periods of heavy precipitation or high gusts. Climate also influences soil erosion. Since water can easily scour away the soil's top layer, heavy precipitation or frequent cyclones increase the likelihood of soil erosion. Lineaments, which can be straight or curved, are geomorphic features associated with geological features such faults and lithological contacts (Argaz et al., 2019). Soil erosion is affected by infiltration and surface runoff, both of which are impacted by the lineament (Mosavi et al., 2020). Lineament can increase the rate of soil erosion. Because rainwater is focused along the linear features and runs swiftly down steep slopes, high lineament density can result in increased surface runoff and soil erosion. This can lead to soil degradation, topsoil loss, decreased soil fertility, and decreased agricultural output. The rate of soil erosion in mountainous regions is significantly affected by surface roughness. Differences in elevation, plant cover, and surface imperfections all contribute to what hydrologists call "roughness of the land surface," which may affect how water and sediment flow through the landscape. By controlling the flow of water and the transport of sediment, it has an effect on the rate and severity of soil erosion (Foster et al., 1985; Levy et al., 1994). Topography, which includes the terrain's form, slope, and other characteristics, has a significant impact on soil erosion. The morphology of hilly landscapes influences the flow of water, the transport of sediment, and the processes of erosion. Understanding the morphology of hilly regions is necessary for implementing effective soil erosion control measures. Consequently, erosion-prone areas can be identified and protected using best management practices (Ghosh & Maiti, 2021a).

2.3. Data driven approaches for soil susceptibility mapping

2.3.1. Support vector machine

SVMs, which are grounded in statistical learning theory, have seen

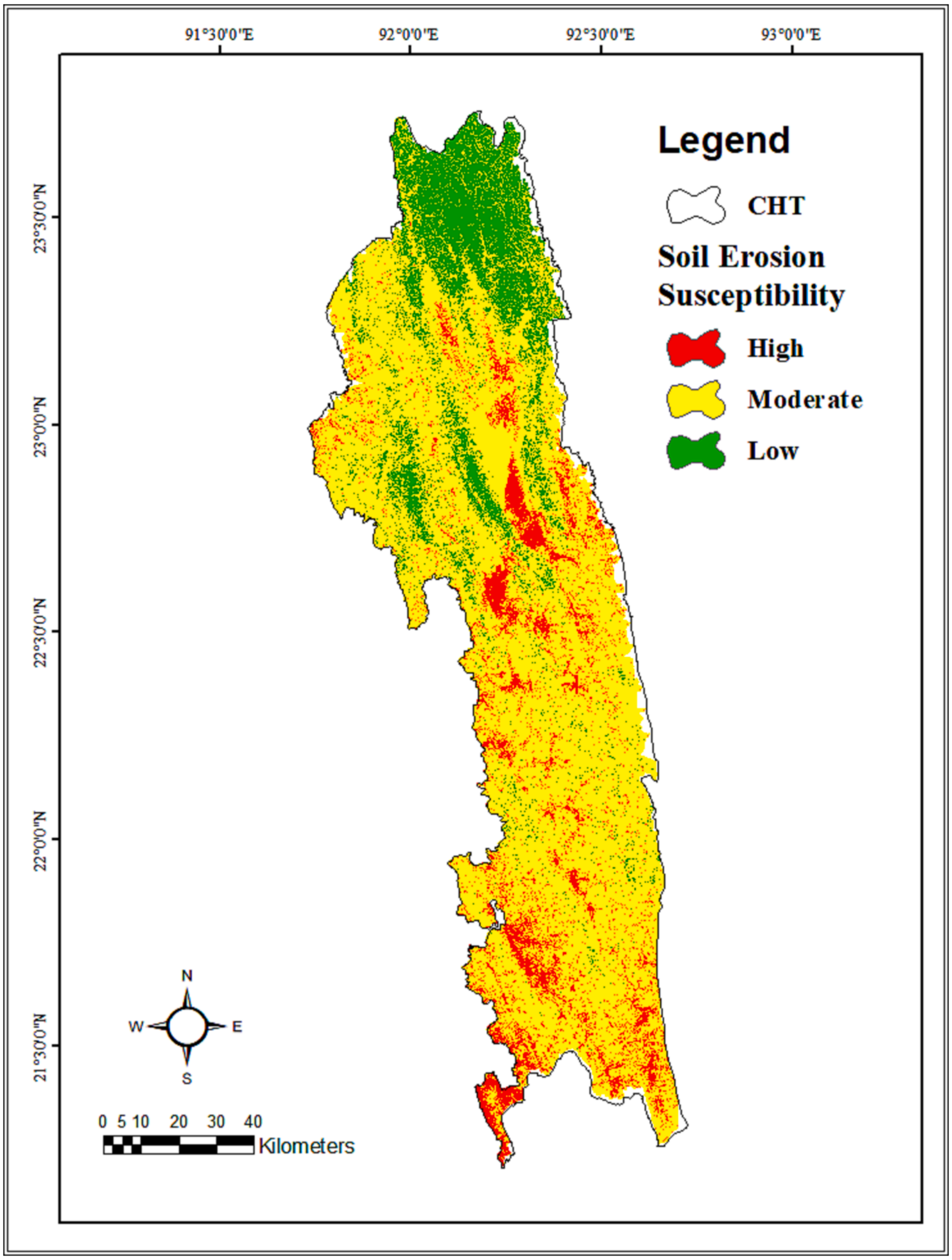

Fig. 8. Soil Susceptibility Maps by Knowledge-based Approach (AHP).

considerable application as a data mining tool for a wide range of difficult classification and regression issues. The primary intention of SVMs was to identify the best linear hyperplane for distinguishing between two classes, making them a kind of binary classifier (Vapnik, 1999). In the case of binary classification problems where samples are linearly separable, SVMs attempt to locate a separating hyperplane in the feature space that maximises the distance between positive and negative samples (Pisner & Schnyer, 2019). Based on statistical learning theory and the notion of structural risk reduction, SVM is a machine learning algorithm (Nhu et al., 2020; Tran Van & Prakash, 2020). Using a kernel function and the optimum classification hyperplane are the two main concepts of support vector machines (Yao et al., 2008). Support vectors (H1 and H2) are lines perpendicular to the classification line (H) that pass through the locations on the samples that are most in close proximity to the line (the dots and squares in). The labelling margin is the distance between the two groups. A support vector machine (SVM) is a popular machine learning tool for making accurate predictions with little information. In this analysis, we use support vector machines to map soil erosion vulnerability. It explains how SVM works and how it may be used to create a soil erosion risk map. Three different approaches to landslip susceptibility mapping are then compared with the SVM method: the correlation and regression tree, artificial neural networks, and random forests. Future research directions are discussed, and a review of the use of SVM to landslip susceptibility assessment and mapping is presented. In this data-driven and machine learning-based procedure, the data is divided into two sets: 70 % for training and 30 % for testing.

2.3.2. *Random Forest*

An advanced decision tree model, random forest builds several trees for use in regression and classification analyses. Overfitting is possible in standard DT models since they rely on a single tree for explanatory power. The random forest model was created specifically to deal with this issue. Ghosh & Maiti, 2021 research work highlights the significance

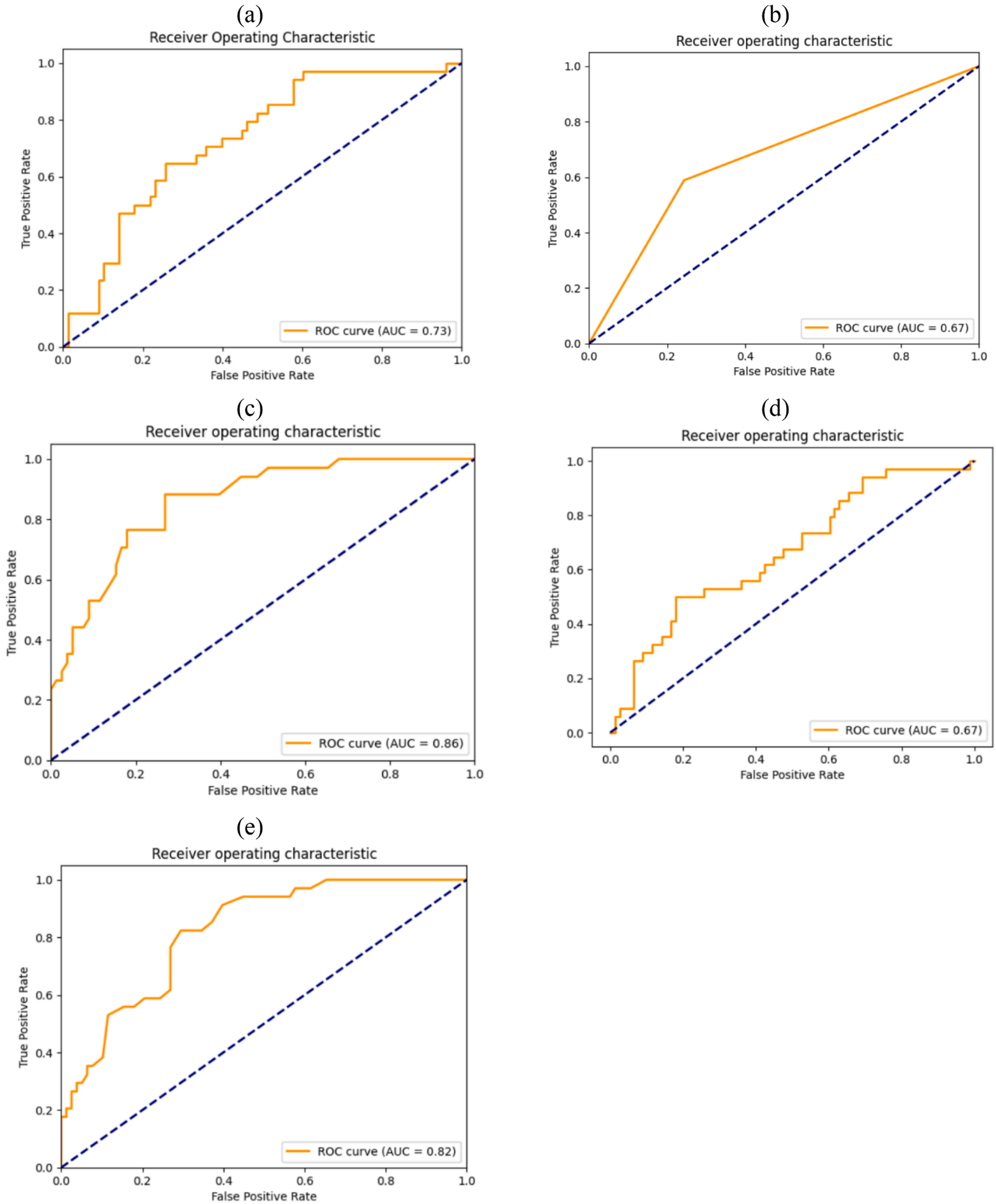

Fig. 9. ROC Curve of Data driven models (a)ANN, (b) CART, (c) RF, (d) SVM (e) AHP.

of the random forest model's inputs, namely the number of trees and the predictive parameters at each node. Classification and regression variables, interactions, and aggregated data may all benefit from this method (Rahmati et al., 2017). The RF model uses several decision tree models instead of just one, and it can handle both continuous and discrete data. (Avand et al., 2019; Sun et al., 2021, Mosavi et al., 2020, Bag et al., 2022). The geographical correlation between avalanche occurrences may be better understood with the help of a large number of decision trees generated using the Random Forest ensemble method of machine learning. It is effective because it trains numerous decision trees, each of which may be used for either classification or regression (Cheng et al., 2018; Jin et al., 2020; Kim et al., 2018; Liaw & Wiener, 2002). The class is determined via a decision tree built as part of the classification method (Dharumarajan et al., 2017). The dependent

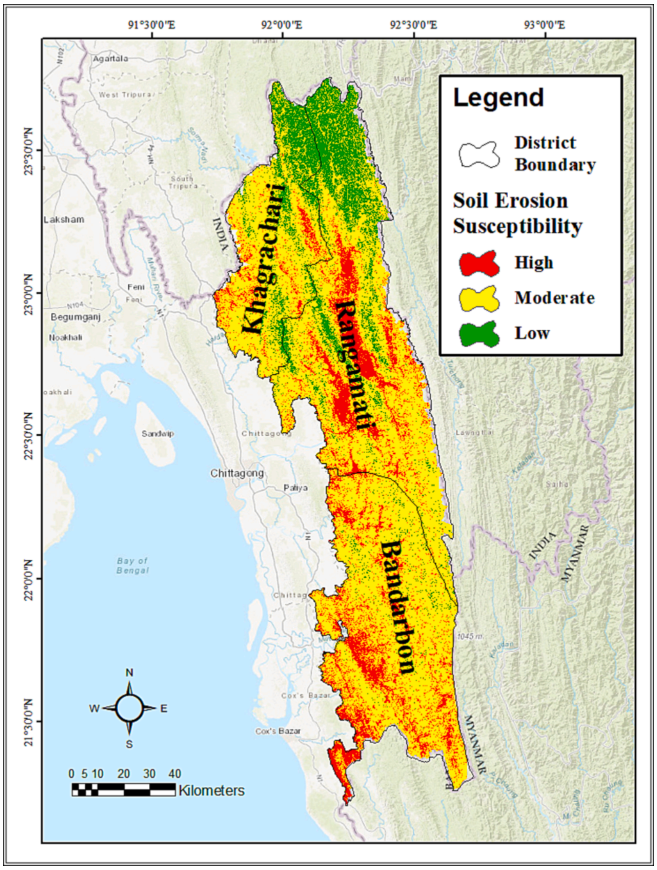

Fig. 10. District wise Soil Erosion Susceptibility by best model (RF.

Table 4
Percentage of susceptibility categories in different districts by best model (RF).

District	High		Moderate		Low	
	Area (sq. km)	%	Area (sq. km)	%	Area (sq. km)	%
Bandarban	972.26	21.71	3355.56	74.92	151.19	3.38
Rangamati	461.55	16.79	1824.60	66.37	462.85	16.84
Khagrachari	497.56	8.14	4520.08	73.91	1098.36	17.96

variable is estimated by taking the mean of the findings from the regression procedure (Kim et al., 2018). The machine learning process employs a total of 100 estimators, with 70 % of the data allocated for training purposes and the remaining 30 % for testing.

2.3.3. Artificial neural network

Artificial neural networks (ANN) are a kind of AI that may be used to statistically identify the patterns of the intricate interactions that form the basis of geo environmental information. It's malleable because it can roughly estimate the linearity or nonlinearity of a connection between dependent and covariate or factorial variables and a complicated data structure. For rapid decision making, the neural network employs a method wherein it develops several approximations and tries modifications to build a better approximation depending on user-specified criteria (T. Sarkar & Mishra, 2018). Anomaly detection using ANN is a standard method for avalanche risk mapping. The typical architecture of an ANN consists of three layers: input, hidden, and output. Each input value is then multiplied by the total mass of the assembly at each calculation node (Zhao et al., 2010). A neuron-specific restriction named bias is then applied to the combined yields in order to bring them into a reasonable range (Melchiorre et al., 2008). By applying an activation function to this total, the computational node produces output (Rudra & Sarkar, 2023). By minimizing a learning function that represents the gap between observations and ANN output during training, a non-linear optimization training approach is utilized to construct weights and biases (Nhu et al., 2020). The data-driven and machine learning based procedure utilizes 100 hidden layers for performing the process. 70 % of the data is allocated for training purposes, while the remaining 30 % is reserved for testing.

2.3.4. Correlation and regression tree

CART is a popular data extraction method that uses recursive binary division to swiftly analyse big data. Get started using a dataset that includes both the independent factors and the variable you want to forecast. Utilizing the CART algorithm, build a decision tree. The data is partitioned recursively based on predictor variables, and the best predictor variable and split point that optimizes the correlation or regression relationship within each subset are chosen. Whether the dependent variable is continuous (regression) or categorical (classification) determines the dividing criteria. For regression, minimize the variance within each subgroup, and for classification, maximize the homogeneity or purity of each subdivision based on the target variable. The data is subdivided repeatedly into smaller subsets based on the selected variable and split point. This procedure is repeated until a predetermined condition, such as a maximal tree depth or a minimal number of samples in each subgroup, is met. Using the created tree, new data points can be predicted by following the predictor variable values down the tree. The prediction is made by averaging the target variable values within the leaf node that corresponds to the path of the data point. The resultant tree structure illuminates the connections between predictor and target variables. The decision criteria at each node can be read to comprehend how various variables affect the prediction (Saha et al., 2004). In this data-driven and machine learning-based procedure, the dataset is divided into two subsets: 70 % of the data is allocated for training purposes, while the remaining 30 % is reserved for testing.

2.4. Knowledge-based approaches for soil susceptibility mapping

2.4.1. Analytical Hierarchy process

Using a variety of criteria, AHP narrows down the options for making a choice and helps choose the best one. Evaluation of potential solutions to a problem by giving each one a number rating depending on how well it satisfies the decision maker's criteria. The potential prediction accuracy of AHP methods and other machine learning techniques has been reported on in many research proving the dependability of machine learning (Tolche et al., 2021). AHP is still one of the most renowned analytical techniques for difficult decision-making process because of its flexibility and applicability (Sinshaw et al., 2021). A decision-making scenario may be described using an AHP hierarchy with numerous levels. To assign values to the variables that characterise the site's suitability, the Analytical Hierarchy Process (AHP) uses a pairwise comparison matrix with a scale of relative significance (Raisi et al., 2014; Tairi et al., 2019).

2.5. Validation of the models (ROC curve and AUC)

When testing algorithmic learning models for usage in susceptibility mapping for hazards associated with the environment, the receiver operating characteristic (ROC) curve is a common quantitative validation tool (Arabameri et al., 2018; Jaafari & Pourghasemi, 2019; Nhu et al., 2020; Pradhan & Kim, 2020) by analyzing the consistency between model outputs and ground truth data. The ROC curve has been used in a number of case studies to depict the compromise between sensitivity and specificity. Competence and ambiguity of the examined models are shown by the change in AUC from 0.5 to 1 (Ghorbanzadeh et al., 2020; Pourghasemi et al., 2020).

The test's capacity to distinguish between flooded and unflooded areas was measured using the area under the receiver operating characteristic (ROC) curve. The value of a test is often measured by its area under a receiver operating characteristic (ROC) curve, with a bigger area indicating more value. A continuous random variable display style XX, which is the instance's "score" (for example, the estimated probability in logistic regression), is often used to produce the class prediction for each instance in binary classification. Instances are classified as "positive" when display style X > TX > T and as "negative" when the opposite is true, where display style TT is the threshold parameter. If the instance is of the "positive" class, then display style XX conforms to the probability density of display style f 1(x)f 1(x), and if it is not, then display style f 0 (x)f 0(x) is used (Biswas et al., 2012).

The overall methodological framework is shown in (Fig. 2).

3. Results

3.1. Descriptions of parameters

From Fig. 3, the analysis of the slope parameter reveals that the northern portion of our research area exhibits a greater degree of steepness, consequently leading to a higher incidence of erosion within that particular region. It has been determined that the southern section exhibits a greater degree of steepness, as indicated by the Elevation parameter. The rise in soil erosion is a direct consequence of higher precipitation. The parameter inside a curvature map provides information regarding the direction of slope, the location of elevated terrain, the presence of depressions, and the identification of convex and concave regions. The regions located in the northern and southern portions of the map have a greater prevalence of higher convex areas, which consequently experience a higher degree of soil erosion.

The drainage density parameter exhibits a greater drainage density within the middle region of the land, thereby leading to an elevated potential for soil erosion. Based on the parameter map for Topographic Wetness Index (TWI), it may be inferred that a location with a high TWI value signifies saturation, hence suggesting a heightened susceptibility to erosion within that area. The transverse wave impedance (TWI) exhibits a larger value throughout the center part. In the southern region of the Chittagong hill tracts, the length of stream linkages is observed to be greater, which can be attributed to the higher levels of soil erosion in this area. Flow accumulation exhibits significant values in certain areas, as evidenced by the flow accumulation map. Soil erosion is a prevalent occurrence in areas characterized by high flow rates. According to the watershed parameter map, the catchment area has a larger extent in the southern region of the Chittagong hill tracts. This observation implies a higher degree of erosion in the specified area. A positive correlation exists between stream order and soil erosion within the Stream order parameter (Fig. 4).

Fig. 5 denotes, Areas with a higher density of vegetation see reduced erosion rates. Based on the analysis of Normalized Difference Vegetation Index (NDVI) data, it is evident that the southern regions of our designated research area exhibit a higher prevalence of vegetative cover, hence indicating a reduced occurrence of erosion in those areas. A resemblance is observed in the Land Use and Land Cover (LULC) analysis. The density of vegetation increases as one moves towards the southern region. Consequently, the severity of erosion is reduced. Based on the statistic known as the Soil Brightness Index, it can be observed that the southern region has a comparatively elevated Soil Brightness Index. A high SBI score indicates that the soil exhibits characteristics consistent with a rock type composition. The presence of rocky soil contributes to the stability of the ground, making it less susceptible to erosion.

The roughness parameter exhibits a lower degree of roughness in the central region. It has been determined that the presence of less rocky terrain leads to an increase in erosion, as evidenced by the utilization of the lineament density measure. It can be inferred from the Soil group parameter that the entire region exhibits uniform brown/grey soil characteristics. The selection was made due to its vital role in my research. Ligaments exhibit greater thickness in the vicinity of the Chittagong hill tracts, an area characterized by heightened erosion. A steeper slope of the hill is observed across the entire area in the Morphology parameter. The increased gradient of the hill contributes to heightened soil erosion (Fig. 6).

3.2. Soil susceptibility mapping by data driven approach

With eighteen soil erosion control parameters as training datasets, this research produced four SESM using SVM, CART, ANN, and RF machine learning models (Fig. 7). Each SESM was then assigned to one of three susceptibility groups based on their degree of sensitivity to SE: low, moderate, or high. We found that a large percentage of the basin is vulnerable to soil erosion, suggesting that it may be a problem in this area. According to the SESM, the basin's southern, south-eastern, western, and southwestern regions have high, moderate, moderate, and high risk, respectively. Where there is a high concentration of both uncultivated and cultivated land, the slope and elevation, soil erosion is moderate.

According to the SVM-generated SESM (Table 2), 17.69 % of the area is comprised of high erosion zones, while 70.60 % is comprised of moderate zones. The remaining 11.71 % falls within the zone of low soil erosion. The CART model designated 14.03 % as low-risk, 698.5 % as moderate-risk, and 16.1 % as high-risk. On the other hand, the ANN SESM showed that most of the region (70.85 %) has a moderate soil erosion potential, followed by 12.03 % to the low susceptible category and 17.12 % in the high soil erosion risk zone. The RF model predicted that 71.55 percent of the region will be eroded. Only 16.59 percent of the terrain was considered high, while 11.54 percent was considered low (Table 3).

3.3. Soil susceptibility mapping by knowledge-based approach

3.3.1. Weight of the soil erosion parameters by AHP

AHP-generated SESM (Fig. 8) indicates that the northern side has a low potential soil erosion zone, whereas the other sides have high and moderate potential zones, respectively. According to the findings, 14.19 % of the entire land is very resistant to soil erosion due to its plant cover. In contrast, 74.35 % of the land area is at moderate risk for soil erosion, and this zone includes both moderate and high elevation locations. There is a high risk of soil erosion on 11.46 percent of the land.

3.4. Validation of models by ROC and AUC (data driven approach)

Soil erosion susceptibility mapping rigor was measured using the ROC-AUC metric. SVM and RF both have metric values of 0.67, whereas CART and ANN both have values of 0.86 and ANN has a value of 0.73. This degree of agreement between the distribution of observed erosional zones and the final anticipated maps is indicative of a moderate to outstanding projection capability across all models. Each model came within a small margin of error of what really occurred. According to the findings, SVM, CART, and ANN all achieve equivalent levels of accuracy. While the ANN, SVM, and CART models were all useful in some ways, the AUC analysis shows that the data driven RF model is the best choice for mapping susceptible soil erosion areas in this particular research region. The AUC values for RF and AHP are 0.86 and 0.82, respectively, when compared to those of the Knowledge-Based Model and the Data-Driven Model. The model and the final forecasted maps of the study area show a high degree of agreement in the settings of existing erosional zones. The AUC suggests that the RF model has more promise than the AHP technique for mapping soil erosion sensitivity in the research area, despite the AHP model's superior predictive performance (Fig. 9).

3.5. District wise soil erosion susceptibility by best model (RF)

According to research utilizing the RF model (Fig. 10 & Table 4), nearly three-quarters (74.92 percent) of Bandarban lies within a moderate soil erosion zone characterized by high and moderate elevation and a small (3.38 percent) region susceptible to soil erosion. In contrast, Rangamati has a greater concentration of water bodies and 66.37 percent of its land area is covered by a zone of moderate soil erosion. And only 16.79 % and 16.84 % of the land is vulnerable to soil erosion. In contrast, 73.91 %, 17.96 %, and 8.14 % of Khagrachari, respectively, lie within the moderate, low, and high soil erosion zones.

4. Discussion

Numerous researchers and scientists have utilized extensive modeling to determine accurate methods for mapping soil erosion and, ultimately, how to reduce and eventually stop it. Previous research in CHT has mapped landslide susceptibility, but not soil erosion susceptibility. The alteration in soil quality resulting from soil pollution and soil erosion has a substantial impact on the ecosystem (Alqadhi et al., 2022; Mallick et al., 2022). By using a Geographic Information System (GIS)-based multi-criteria decision technique, and considering eleven distinct variables, The resulting composite map displays the varying degrees of soil erosion in Chitral, Pakistan, categorized into five distinct classes: very high, high, medium, low, and very low. The studied area exhibits a prevalence of 13 % and 18 % for very high and high erosion, respectively, indicating a significant risk of soil erosion in the region. The primary components impacting the soil erosion process have been identified as elevation, slope, curvature, normalized difference water index (NDWI), and rainfall (Aslam et al., 2021). Using the RUSLE method, Rahman (2021) estimates that woods make up around 69,803 ha (or about 20 %) of the total area in the watershed of the study region. Soil erosion rates in high-importance regions are between 49.20 and 86.70 kg/ha/yr. Most soil is lost from forested regions, then from towns and roadways. Agricultural fields and cultivated lands are often located on low-lying regions with gradients ranging from 0 to 19 %, while woods are typically found on steep slopes ranging from 37 to 121 %. Rabby (2020) uses machine learning to determine an increase in the high susceptibility zone of 28.7 and 43.1 % for planned and simulated LULC situations, respectively. Also, from (Rabby & Li, 2020) Frequency ratio (FR) and evidentiary belief function (EBF) are two types of bivariate models; by combining them with knowledge-based AHP and multivariate logistic regression, we may increase the accuracy of our landslide susceptibility maps in CHT. In this study, our focus is narrowed to the examination of soil erosion susceptibility. Our findings indicate that among data-driven and knowledge-based models, the random forest model proves to be the most successful for accurately mapping this variable. Based on RF's findings, it is indicated that a considerable proportion of the entire region, specifically 71.55 percent, is susceptible to experiencing substantial soil erosion. The regions characterized by higher elevation and lower elevation accounted for 16.91 percent and 11.4 percent of the total land area, respectively. Upon analyzing the district-specific data, it is evident that a significant portion of Bandarban (specifically, 74.92 percent) is situated within a zone characterized by a moderate risk of soil erosion. This moderate risk is attributed to the district's considerable elevation, which is classified as high or moderate. Conversely, only 21.71 percent and 3.38 percent of the district's territory are categorized as being at greater and lower risk levels of soil erosion, respectively. In contrast, a significant portion of Rangamati, around 66.37 percent, is characterized by a moderate soil erosion zone and a substantial presence of water bodies. The regions with the highest susceptibility to soil erosion encompass a mere 16.79 % and 16.84 % of the total land area. In contrast, the region of Khagrachari exhibits varying degrees of soil erosion, with moderate erosion being 7.391 % of the total, low erosion accounting for 17.96 %, and severe erosion representing 8.140 %.

5. Conclusion

Using data-driven machine learning approaches and knowledge-based processes, this research aimed to locate areas of soil erosion in the Chittagong Hill Tracts. If put into practice, the models developed in these studies may significantly reduce costs and improve efficiency. Therefore, the RF, SVM, CART, and ANN models should be used, with the user choosing the appropriate parameters according to the specifics of the region's geography and climate. The RF model provides the best fit, performance, and prediction when compared to the other models (AUCs = SVM = 67 %, ANN = 73 %, RF = 86 %, AHP = 82 %, and CART = 67 %). On top of that, it claims that when compared to the knowledge-based model, the soil viability mapping produced by the data-driven approach is more accurate. All models have inherent flaws, but they all provide useful information that may be used to better manage land resources in the Chittagong Hill Tracts. Soil erosion is more common in the highlands of Bangladesh's CHT watershed, whereas it is less of a problem in the lowlands. CHT regional development and land use planning may benefit greatly from the study's susceptibility maps. The majority of the western CHT was classified as low susceptible on the susceptibility maps. Strict land-use planning should be adopted in high and very high vulnerability zones, with authorities and stakeholders taking precautionary steps for development activities like road building. The findings of this study would benefit SDG Goals related to "Life on Land," "Climate Action," "Zero Hunger," and "Sustainable Cities and Communities." Soil erosion contributes to climate change in numerous ways, including the loss of arable land, a decline in agricultural output, and an increase in sedimentation in aquatic bodies. Soil erosion is a significant contributor to climate change, but this study mitigates this effect by paving the way for more precise erosion control strategies and environmentally responsible land management. Significant losses in agricultural production and hazards to food security are a result of soil erosion. The findings may inform concerted action to preserve farmland, enhance sustainable agricultural practices, and advance SDG 2's objective of ending world hunger. Goal 15 of the Sustainable Development Goals, "Life on Land," is concerned with the management and conservation of terrestrial ecosystems, and thus has a direct consequence on the research presented here. By mapping soil erosion susceptibility, the initiative aims to identify vulnerable areas and provide crucial information for land management measures to halt further degradation and promote sustainable land use in the CHT. Both urban and rural regions are designated CHT. This research contributes to Sustainable Development Goal 11 by encouraging informed urban planning and land use decisions, which in turn promotes sustainable development and resilient communities in the region. In order to address the issue of soil erosion in the Chittagong Hill Tracts region of Bangladesh, it is imperative to adopt a comprehensive and diverse strategy. To begin with, it is imperative to advocate for the extensive implementation of terracing and contour farming practices as a means to decelerate water runoff and mitigate soil erosion on inclined terrains. Furthermore, it is imperative to give precedence to reforestation initiatives that focus on utilizing indigenous plant species. This approach serves the purpose of stabilizing the soil and mitigating the risk of erosion. Furthermore, it is imperative to involve local communities in watershed management initiatives in order to collaboratively tackle erosion concerns and establish sustainable land utilization strategies. In conclusion, it is imperative to implement rigorous rules pertaining to activities such as logging and land usage in order to mitigate erosion-prone practices. This measure is crucial for safeguarding the long-term sustainability of the region's delicate ecosystem and the welfare of its residents.

Funding

None.

Ethical approval

The authors declare No ethical approval required. Ethical approval for this type of study is not required by our institute.

CRediT authorship contribution statement

Halima Sadia: Conceptualization, Methodology, Investigation, Data curation, Formal analysis, Software, Visualization, Writing – original draft. **Showmitra Kumar Sarkar:** Supervision, Conceptualization, Methodology, Writing – review & editing. **Mafrid Haydar:** Investigation, Visualization, Writing – review & editing.

Declaration of Competing Interest

The authors declare that they have no known competing financial interests or personal relationships that could have appeared to influence the work reported in this paper.

Data availability

Data will be made available on request.

References

Abad-Segura, E., González-Zamar, M.D., Vázquez-Cano, E., López-Meneses, E., 2020. Remote sensing applied in forest management to optimize ecosystem services: Advances in Research. Forests 11 (9). https://doi.org/10.3390/f11090969.

Ahmad, F., Goparaju, L., 2017. Soil and Water Conservation Prioritization Using Geospatial Technology – a Case Study of Part of Subarnarekha Basin, Jharkhand, India. AIMS Geosci. 3 (3), 375–395. https://doi.org/10.3934/geosci.2017.3.375.

Ahmed, A., Nawaz, R., Woulds, C., Drake, F., 2020. Influence of hydro-climatic factors on future coastal land susceptibility to erosion in Bangladesh: a geospatial modelling approach. J. Geovisual. Spat. Anal. 4 (1) https://doi.org/10.1007/s41651-020-00050-x.

Al Raisi, S.A.H., Sulaiman, H., Abdallah, O., Suliman, F., 2014. Landfill suitablity analysis using Ahp method and state of heavy metals pollution in selected landfills in Oman. Eur. Sci. J. ESJ 10 (17), 1857–7881. https://eujournal.org/index.php/esj/article/view/3565.

Alqadhi, S., Mallick, J., Talukdar, S., Ahmed, M., Khan, R.A., Sarkar, S.K., Rahman, A., 2022. Assessing the effect of future landslide on ecosystem services in Aqabat Al-Sulbat region, Saudi Arabia. Vol. 113, Issue 1. In: Natural Hazards. Springer, Netherlands. https://doi.org/10.1007/s11069-022-05318-7.

Amarakul, V. (2001a). GIS application on geological characteristics as the predicting for soil erosion in Khaew Noi watershed, Phitsanulok province. *22nd Asian Conference on Remote Sensing., November*, 5–9.

Amarakul, V. (2001b). GIS application on geological characteristics as the predicting for soil erosion in Khaew Noi watershed, Phitsanulok province. *22nd Asian Conference on Remote Sensing., November*, 5–9.

Arabameri, A., Rezaei, K., Pourghasemi, H.R., Lee, S., Yamani, M., 2018. GIS-based gully erosion susceptibility mapping: a comparison among three data-driven models and AHP knowledge-based technique. Environ. Earth Sci. 77 (17), 1–22. https://doi.org/10.1007/s12665-018-7808-5.

Argaz, A., Ouahman, B., Darkaoui, A., Bikhtar, H., Ayouch, E., Lazaar, R., 2019. Flood hazard mapping using remote sensing and GIS Tools: A case study of Souss Watershed. J. Mater. Environ. Sci 10 (2), 170–181. http://www.jmaterenvironsci.com.

Aslam, B., Maqsoom, A., Salah Alaloul, W., Ali Musarat, M., Jabbar, T., Zafar, A., 2021. Soil erosion susceptibility mapping using a GIS-based multi-criteria decision approach: Case of district Chitral, Pakistan. Ain Shams Eng. J. 12 (2), 1637–1649. https://doi.org/10.1016/j.asej.2020.09.015.

Avand, M., Mohammadi, M., Mirchooli, F., Kavian, A., Tiefenbacher, J.P., 2023. A new approach for smart soil erosion modeling: integration of empirical and machine-learning models. Environ. Model. Assess. 28 (1), 145–160. https://doi.org/10.1007/s10666-022-09858-x.

Bag, R., Mondal, I., Dehbozorgi, M., Bank, S.P., Das, D.N., Bandyopadhyay, J., Pham, Q. B., Fadhil Al-Quraishi, A.M., Nguyen, X.C., 2022. Modelling and mapping of soil erosion susceptibility using machine learning in a tropical hot sub-humid environment. J. Clean. Prod. 364 (November 2021), 132428 https://doi.org/10.1016/j.jclepro.2022.132428.

Bai, Z. G., Dent, D. L., Olsson, L., & Schaepman, M. E. (2008). Proxy global assessment of land degradation. In *Soil Use and Management* (Vol. 24, Issue 3, pp. 223–234). https://doi.org/10.1111/j.1475-2743.2008.00169.x.

Bai, Z. G. (2006). *Assessing land degradation in the Chittagong Hill Tracts, Bangladesh, using NASA GIMMS*.

Berberoglu, S., Cilek, A., Kirkby, M., Irvine, B., Donmez, C., 2020. Spatial and temporal evaluation of soil erosion in Turkey under climate change scenarios using the Pan-European Soil Erosion Risk Assessment (PESERA) model. Environ. Monit. Assess. 192 (8) https://doi.org/10.1007/s10661-020-08429-5.

Biswas, A., Alamgir, M., Haque, S.M.S., Osman, K.T., 2012. Study on soils under shifting cultivation and other land use categories in Chittagong Hill Tracts, Bangladesh. J. Forest. Res. 23 (2), 261–265. https://doi.org/10.1007/s11676-011-0216-2.

Chakrabortty, R., Pal, S.C., Sahana, M., Mondal, A., Dou, J., Pham, B.T., Yunus, A.P., 2020. Soil erosion potential hotspot zone identification using machine learning and statistical approaches in eastern India. In: Natural Hazards, Vol. 104, Issue 2. Springer, Netherlands. https://doi.org/10.1007/s11069-020-04213-3.

Cheng, Z., Lu, D., Li, G., Huang, J., Sinha, N., Zhi, J., Li, S., 2018. A random forest-based approach to map soil erosion risk distribution in hickory plantations in Western Zhejiang Province, China. Remote Sens. (Basel) 10 (12). https://doi.org/10.3390/rs10121899.

Dharumarajan, S., Hegde, R., Singh, S.K., 2017. Spatial prediction of major soil properties using Random Forest techniques - A case study in semi-arid tropics of South India. Geoderma Reg. 10, 154–162. https://doi.org/10.1016/j.geodrs.2017.07.005.

Farid, A. T. M. , Iqbal, A. , & Karim, Z. (1995). *Soil erosion in the Chittagong hill tract and its impact on nutrient status of soils [in Bangladesh]*. Soil Erosion in the Chittagong Hill Tract and Its Impact on Nutrient Status of Soils [in Bangladesh]. https://agris.fao.org/agris-search/search.do?recordID=BD9525011.

Foster, G. R., Young, R. A., Romkens, M. J. M., & Onstad, C. A. (1985). *9 Processes of Soi I Erosion by Water*.

Ghorbanzadeh, O., Shahabi, H., Mirchooli, F., Valizadeh Kamran, K., Lim, S., Aryal, J., Jarihani, B., Blaschke, T., 2020. Gully erosion susceptibility mapping (GESM) using machine learning methods optimized by the multi–collinearity analysis and K-fold cross-validation. Geomat. Nat. Haz. Risk 11 (1), 1653–1678. https://doi.org/10.1080/19475705.2020.1810138.

Ghosh, A., Maiti, R., 2021. Soil erosion susceptibility assessment using logistic regression, decision tree and random forest: study on the Mayurakshi river basin of Eastern India. Environ. Earth Sci. 80 (8) https://doi.org/10.1007/s12665-021-09631-5.

Halefom, A., Teshome, A., 2019. Modelling and mapping of erosion potentiality watersheds using AHP and GIS technique: a case study of Alamata Watershed, South Tigray, Ethiopia. Modeli. Earth Syst. Environ. 5 (3), 819–831. https://doi.org/10.1007/s40808-018-00568-6.

Hasan, M.K., Ashraful Alam, A.K.M., 2006. Land degradation situation in Bangladesh and role of agroforestry. J Agric Rural Dev 4 (2), 19–25.

Hossain, F., Sadeak, S., & Gazi, M. Y. (2022). Quantitative soil erosion risk assessment due to rapid urbanization in the Cox's Bazar district and Rohingya refugee camps in Bangladesh. https://doi.org/10.21203/rs.3.rs-1485047/v1.

Huq, S. M. I., Uddin, J., & Shoaib, M. (2013). *The Soils of Bangladesh World Soils Book Series*. http://www.springer.com/series/8915.

Islam, A., & Islam, M. S. (2017). LANDSLIDES IN CHITTAGONG HILL TRACTS AND POSSIBLE MEASURES Comparative Study on the Genetic Diversity of the Vetiver (Vetiveria zizanoides) Ecotypes Available on Brahmaputra-Ganges Flood Plain View project Development of Earthquake Resistant Adobe Structures Using Fiber Reinforced Plaster and Fiber String View project. https://www.researchgate.net/publication/320014168.

Islam, M. R., Mao, S., & Eneji, A. E. (2010). *Status of land degradation and desertification in Bangladesh and the role of agro forestry in their control*. https://www.researchgate.net/publication/260481130.

Jaafari, A., Pourghasemi, H.R., 2019. Factors influencing regional-scale wildfire probability in Iran. In: Spatial Modeling in GIS and R for Earth and Environmental Sciences. Elsevier, pp. 607–619. https://doi.org/10.1016/b978-0-12-815226-3.00028-4.

Jin, Z., Shang, J., Zhu, Q., Ling, C., Xie, W., Qiang, B., 2020. RFRSF: Employee Turnover Prediction Based on Random Forests and Survival Analysis. In: Lecture Notes in Computer Science (Including Subseries Lecture Notes in Artificial Intelligence and Lecture Notes in Bioinformatics). https://doi.org/10.1007/978-3-030-62008-0_35.

Kim, J.C., Lee, S., Jung, H.S., Lee, S., 2018. Landslide susceptibility mapping using random forest and boosted tree models in Pyeong-Chang. Korea. *Geocarto International* 33 (9), 1000–1015. https://doi.org/10.1080/10106049.2017.1323964.

Krishna Bahadur, K.C., 2009. Mapping soil erosion susceptibility using remote sensing and GIS: A case of the Upper Nam Wa Watershed, Nan Province, Thailand. Environ. Geol. 57 (3), 695–705. https://doi.org/10.1007/s00254-008-1348-3.

Levy, G. J., Levin, J., & Shainberg, I. (1994). *Seal Formation and Intertill Soil Erosion*.

Liaw, A., & Wiener, M. (2002). *Classification and Regression by randomForest* (Vol. 2, Issue 3). http://www.stat.berkeley.edu/.

Lohani, S., Baffaut, C., Thompson, A.L., Aryal, N., Bingner, R.L., Bjorneberg, D.L., Bosch, D.D., Bryant, R.B., Buda, A., Dabney, S.M., Davis, A.R., Duriancik, L.F., James, D.E., King, K.W., Kleinman, P.J.A., Locke, M., McCarty, G.W., Pease, L.A., Reba, M.L., Yasarer, L.M.W., 2020. Performance of the Soil Vulnerability Index with respect to slope, digital elevation model resolution, and hydrologic soil group. J. Soil Water Conserv. 75 (1), 12–27. https://doi.org/10.2489/JSWC.75.1.12.

Mallick, J., Alqadhi, S., Talukdar, S., Sarkar, S.K., Roy, S.K., Ahmed, M., 2022. Modelling and mapping of landslide susceptibility regulating potential ecosystem service loss: an experimental research in Saudi Arabia. Geocarto Int. 37 (25), 10170–10198. https://doi.org/10.1080/10106049.2022.2032393.

Mandal, D., Sharda, V.N., 2013. Appraisal of soil erosion risk in the eastern himalayan region of india for soil conservation planning. Land Degrad. Dev. 24 (5), 430–437. https://doi.org/10.1002/ldr.1139.

Mantel, S., & Khan, M. (2006). Chittagong Hill Tracts Improved Natural Resource Management : Report on the National Workshop held in Rangamati Chittagong Hill Tracts Improved Natural Resource Management (CHARM) project View project

BioC4-New integrative sustainable system from C4 photosyntetic miscanthus to biological synthesis of valuable C4 compounds View project. http://www.isric.org.
Mardamootoo, T. (2015). *Developing an index for phosphorus loss from sugarcane soils in Mauritius*.
Melchiorre, C., Matteucci, M., Azzoni, A., Zanchi, A., 2008. Artificial neural networks and cluster analysis in landslide susceptibility zonation. Geomorphology 94 (3–4), 379–400. https://doi.org/10.1016/j.geomorph.2006.10.035.
Mia, M.A., Nasrin, S., Zhang, M., Rasiah, R., 2015. Chittagong, Bangladesh. Cities 48, 31–41. https://doi.org/10.1016/j.cities.2015.05.011.
Mosavi, A., Sajedi-Hosseini, F., Choubin, B., Taromideh, F., Rahi, G., Dineva, A.A., 2020. Susceptibility mapping of soil water erosion using machine learning models. Water (Switzerland) 12 (7), 1–17. https://doi.org/10.3390/w12071995.
Mustafa, M.R.U., Sholagberu, A.T., Yusof, K.W., Hashim, A.M., Khan, M.W.A., Shahbaz, M., 2018. SVM-based geospatial prediction of soil erosion under static and dynamic conditioning factors. MATEC Web of Conferences 203. https://doi.org/10.1051/matecconf/201820304004.
Nearing, M. A., Xie, Y., Liu, B., & Ye, Y. (2017). Natural and anthropogenic rates of soil erosion. In *International Soil and Water Conservation Research* (Vol. 5, Issue 2, pp. 77–84). International Research and Training Center on Erosion and Sedimentation and China Water and Power Press. https://doi.org/10.1016/j.iswcr.2017.04.001.
Nhu, V.H., Shirzadi, A., Shahabi, H., Singh, S.K., Al-Ansari, N., Clague, J.J., Jaafari, A., Chen, W., Miraki, S., Dou, J., Luu, C., Górski, K., Pham, B.T., Nguyen, H.D., Ahmad, B.B., 2020. Shallow landslide susceptibility mapping: A comparison between logistic model tree, logistic regression, naïve bayes tree, artificial neural network, and support vector machine algorithms. Int. J. Environ. Res. Public Health 17 (8). https://doi.org/10.3390/ijerph17082749.
Ouri, A.E., Golshan, M., Janizadeh, S., Cerdà, A., Melesse, A.M., 2020. Soil Erosion susceptibility mapping in kozetopraghi. Land 1–18.
Panwar, A., & Singh, D. (2014). *Watershed Development Prioritization by*. *3*(2), 1597–1601.
Pisner, D.A., Schnyer, D.M., 2019. Support vector machine. In: Machine Learning: Methods and Applications to Brain Disorders. Elsevier Inc. https://doi.org/10.1016/B978-0-12-815739-8.00006-7
Pourghasemi, H.R., Kariminejad, N., Amiri, M., Edalat, M., Zarafshar, M., Blaschke, T., Cerda, A., 2020. Assessing and mapping multi-hazard risk susceptibility using a machine learning technique. Sci. Rep. 10 (1), 1–11. https://doi.org/10.1038/s41598-020-60191-3.
Pradhan, A.M.S., Kim, Y.T., 2020. Rainfall-induced shallow landslide susceptibility mapping at two adjacent catchments using advanced machine learning algorithms. ISPRS Int. J. Geo Inf. 9 (10) https://doi.org/10.3390/ijgi9100569.
Rabby, Y.W., Li, Y., 2020. Landslide susceptibility mapping using integrated methods: A case study in the chittagong hilly areas, bangladesh. Geosciences (switzerland) 10 (12), 1–26. https://doi.org/10.3390/geosciences10120483.
Rahman, N. (2021). Application of the Revised Universal Soil Loss Equation to Application of the Revised Universal Soil Loss Equation to Develop a Management Plan in the Chittagong Hill Tracts Region Develop a Management Plan in the Chittagong Hill Tracts Region of Bangladesh of Bangladesh. https://academicworks.cuny.edu/le_etds/18Discoveradditionalworksat:https://academicworks.cuny.edu.
Rahmati, O., Tahmasebipour, N., Haghizadeh, A., Pourghasemi, H.R., Feizizadeh, B., 2017. Evaluation of different machine learning models for predicting and mapping the susceptibility of gully erosion. Geomorphology 298, 118–137. https://doi.org/10.1016/j.geomorph.2017.09.006.
Rasul, G., Thapa, G.B., Zoebisch, M.A., 2004. Determinants of land-use changes in the Chittagong Hill Tracts of Bangladesh. Appl. Geogr. 24 (3), 217–240. https://doi.org/10.1016/j.apgeog.2004.03.004.
Ravenscroft, P., Burgess, W.G., Ahmed, K.M., Burren, M., Perrin, J., 2005. Arsenic in groundwater of the Bengal Basin, Bangladesh: Distribution, field relations, and hydrogeological setting. Hydrgeol. J. 13 (5–6), 727–751. https://doi.org/10.1007/s10040-003-0314-0.
Razavi-Termeh, S.V., Sadeghi-Niaraki, A., Choi, S.M., 2020. Ubiquitous GIS-based forest fire susceptibility mapping using artificial intelligence methods. Remote Sens. (Basel) 12 (10). https://doi.org/10.3390/rs12101689.
Römkens, M.J.M., Helming, K., Prasad, S.N., 2002. Soil erosion under different rainfall intensities, surface roughness, and soil water regimes. Catena 46 (2–3), 103–123. https://doi.org/10.1016/S0341-8162(01)00161-8.
Roy, S., Pandit, S., Papia, M., Rahman, M.M., Otto Rehder Ocampo, J.C., Razi, M.A., Fraile-Jurado, P., Ahmed, N., Al-Amin Hoque, M., Hasan, M.M., Yeasmin, J., Hossain, M.S., 2021. Coastal erosion risk assessment in the dynamic estuary: The Meghna estuary case of Bangladesh coast. Int. J. Disaster Risk Reduct. 61 https://doi.org/10.1016/j.ijdrr.2021.102364.
Rudra, R.R., Sarkar, S.K., 2023. Artificial neural network for flood susceptibility mapping in Bangladesh. Heliyon 9 (6), e16459.
Saha, S., Kanti Roy, M., Karmakar, C., Saha, S., Chaudhuri, S., 2004. Facies and depositional environment of the dupitila formation, Dupitila hill range, Jaintiapur, Sylhet, Bangladesh. J. Geol. Soc. India 63. https://www.researchgate.net/publication/289688663.
Sarkar, S.K., Ansar, S.B., Ekram, K.M.M., Khan, M.H., Talukdar, S., Naikoo, M.W., Islam, A.R.T., Rahman, A., Mosavi, A., 2022. Developing Robust Flood Susceptibility Model with Small Numbers of Parameters in Highly Fertile Regions of Northwest Bangladesh for Sustainable Flood and Agriculture Management. Sustainability (switzerland) 14 (7), 1–23. https://doi.org/10.3390/su14073982.
Sarkar, T., Mishra, M., 2018. Soil Erosion Susceptibility Mapping with the Application of Logistic Regression and Artificial Neural Network. *Journal of Geovisualization and Spatial*. Analysis 2 (1). https://doi.org/10.1007/s41651-018-0015-9.
Shamshirband, S., Hashemi, S., Salimi, H., Samadianfard, S., Asadi, E., Shadkani, S., Kargar, K., Mosavi, A., Nabipour, N., Chau, K.W., 2020. Predicting Standardized Streamflow index for hydrological drought using machine learning models. Eng. Appl. Comput. Fluid Mech. 14 (1), 339–350. https://doi.org/10.1080/19942060.2020.1715844.
Shit, P.K., Nandi, A.S., Bhunia, G.S., 2015. Soil erosion risk mapping using RUSLE model on jhargram sub-division at West Bengal in India. Model. Earth Syst. Environ. 1 (3), 1–12. https://doi.org/10.1007/s40808-015-0032-3.
Sinshaw, B.G., Belete, A.M., Tefera, A.K., Dessie, A.B., Bizuneh, B.B., Alem, H.T., Atanaw, S.B., Eshete, D.G., Wubetu, T.G., Atinkut, H.B., Moges, M.A., 2021. Prioritization of potential soil erosion susceptibility region using fuzzy logic and analytical hierarchy process, upper Blue Nile Basin, Ethiopia. Water-Energy Nexus 4, 10–24. https://doi.org/10.1016/j.wen.2021.01.001.
Sweeney, B.W., Bott, T.L., Jackson, J.K., Kaplan, L.A., Newbold, J.D., Standley, L.J., Hession, W.C., Horwitz, R.J., 2004. Riparian deforestation, stream narrowing, and loss of stream ecosystem services. PNAS 101 (39), 14132–14137. https://doi.org/10.1073/pnas.0405895101.
Tairi, A., Elmouden, A., Aboulouafa, M., 2019. Soil Erosion Risk Mapping Using the Analytical Hierarchy Process (AHP) and Geographic Information System in the Tifnout-Askaoun Watershed, Southern Morocco. Eur. Sci. J.ESJ 15 (30), 338–356. https://doi.org/10.19044/esj.2019.v15n30p338.
Tehrany, M.S., Shabani, F., Javier, D.N., Kumar, L., 2017. Soil erosion susceptibility mapping for current and 2100 climate conditions using evidential belief function and frequency ratio. Geomat. Nat. Haz. Risk 8 (2), 1695–1714. https://doi.org/10.1080/19475705.2017.1384406.
Tolche, A.D., Gurara, M.A., Pham, Q.B., Anh, D.T., 2021. Modelling and accessing land degradation vulnerability using remote sensing techniques and the analytical hierarchy process approach. Geocarto Int. 1–21. https://doi.org/10.1080/10106049.2021.1959656.
Tran Van, Q., Prakash, I., 2020. Prediction of soil loss due to erosion using support vector machine model. Vietnam J. Earth Sci. 42 (3), 247–254. https://doi.org/10.15625/0866-7187/42/3/15050.
UNICEF. (2019). *MANY TRACTS ONE COMMUNITY*. www.unicef.org.bd.
Vapnik, V.N., 1999. An overview of statistical learning theory. IEEE Trans. Neural Netw. 10 (5), 988–999. https://doi.org/10.1109/72.788640.
Vemu, S., Udayabhaskar, P., 2010. An integrated approach for prioritization of reservoir catchment using remote sensing and geographic information system techniques. Geocarto Int. 25 (2), 149–168. https://doi.org/10.1080/10106040903015798.
Xiao, L., Li, G., Zhao, R., Zhang, L., 2021. Effects of soil conservation measures on wind erosion control in China: A synthesis. Sci. Total Environ. 778, 146308 https://doi.org/10.1016/j.scitotenv.2021.146308.
Xu, C., Xu, X., Yao, Q., Wang, Y., 2013. GIS-based bivariate statistical modelling for earthquake-triggered landslides susceptibility mapping related to the 2008 Wenchuan earthquake, China. Q. J. Eng. Geol. Hydrogeol. 46 (2), 221–236. https://doi.org/10.1144/qjegh2012-006.
Yao, X., Tham, L.G., Dai, F.C., 2008. Landslide susceptibility mapping based on Support Vector Machine: A case study on natural slopes of Hong Kong. China. *Geomorphology* 101 (4), 572–582. https://doi.org/10.1016/j.geomorph.2008.02.011.
Zhao, Z., Yang, Q., Benoy, G., Chow, T. L., Xing, Z., Rees, H. W., & Meng, F.-R. (2010). *Using artificial neural network models to produce soil organic carbon content distribution maps across landscapes*.